

## Monitoring grassland degradation and restoration using a novel climate use efficiency (NCUE) index in the Tibetan Plateau, China

Ru An<sup>a</sup>, Ce Zhang<sup>b,c,\*</sup>, Mengqiu Sun<sup>a</sup>, Huilin Wang<sup>d,\*</sup>, Xiaoji Shen<sup>a,e</sup>, Benlin Wang<sup>a</sup>, Fei Xing<sup>a</sup>, Xianglin Huang<sup>a</sup>, Mengyao Fan<sup>a</sup>

<sup>a</sup> School of Hydrology and Water Resources, Hohai University, China

<sup>b</sup> Lancaster Environment Centre, Lancaster University, UK

<sup>c</sup> UK Centre for Ecology & Hydrology, Library Avenue, Lancaster, UK

<sup>d</sup> Department of Geography Information Science, Nanjing University, China

<sup>e</sup> Department of Civil Engineering, Monash University, Australia

### ARTICLE INFO

#### Keywords:

Grassland degradation and restoration

RUE

NCUE

IMF

TRHR

Tibetan Plateau

### ABSTRACT

Grassland degradation is one of the most pressing challenges in natural environment and anthropogenic society. However, there is yet no effective approach for monitoring the spatio-temporal pattern of large-scale grassland degradation. In particular, the research on grassland changes in the harsh natural environment such as the Qinghai-Tibet Plateau is still in its infancy due to complexity, and it is extremely difficult for humans to reach these remote areas. The annual changes in the grassland biomass might be the results of climate fluctuations or grassland degradation. To test the hypothesis, the impact of inter-annual climate fluctuations needs to be considered when monitoring the grassland degradation based on spatio-temporal change of grassland biomass. In this paper, we propose a Novel Climate Use Efficiency index (NCUE) by considering rainfall, temperature, sunlight time, wind speed, surface temperature, accumulated temperature, time lag effect, light, temperature and water suitability and their coordination climatic factors that mainly affect vegetation growth comprehensively, to monitor grassland change suitable for cold and dry climate characteristics of the Qinghai-Tibet Plateau, and to reduce the effect of inter-annual variability of grassland productivity caused by climate fluctuation. As a consequence, grassland degradation monitoring could be more accurate and objective than existing ecological indicators. Our experiments show that the slope of NCUE over 31 years from 1982 to 2012 is 0.0028, showing a recovery trend in grassland. Degradation and restoration of grassland exist at the same time, and their proportions are 20.49% and 23.89%, respectively. By comparing with in-situ measurements in 2013 and 2009, 68% consistency was achieved with our prediction, and the 70% consistency is achieved by comparing with the positive and negative change trend of accumulated NDVI during the growing season. Moreover, the comparative analysis of land use/cover changes (LUCC) from 1990 to 2010 shows 69% of consistency. The ratio of the area of grassland significantly degradation and recovered predicted by NCUE change trend is 1.41% and 1.43%, respectively. It occupies a very small area of the study area. Yet, that predicted by NDVI change trend is 42.17% and 31.90%, respectively, and about 70% of the area is detected as drastic changes. It shows that NDVI is sensitive to climate fluctuations, while NCUE reduces the impact of climate fluctuations, reflecting change of grassland being affected by human activities and long-term climate change. The novel NCUE has great potential and utility to minimize the impact of climate fluctuation and reflect grassland changes over space and time quantitatively. Such ecological index provides a new understanding of spatial and temporal patterns of grassland degradation in the Three River Headwaters Region (TRHR) at the same time.

### 1. Introduction

Grasslands are one of the most important parts of natural ecosystems.

Grassland degradation refers to significant changes in the composition, structure, and function of grassland ecosystems influenced by human activities or climate-related natural factors. Grassland degradation is

\* Corresponding authors.

E-mail addresses: [c.zhang9@lancaster.ac.uk](mailto:c.zhang9@lancaster.ac.uk) (C. Zhang), [huilin\\_wang@163.com](mailto:huilin_wang@163.com) (H. Wang).

<https://doi.org/10.1016/j.ecolind.2021.108208>

Received 6 April 2021; Received in revised form 10 September 2021; Accepted 11 September 2021

Available online 14 September 2021

1470-160X/© 2021 The Authors. Published by Elsevier Ltd. This is an open access article under the CC BY license (<http://creativecommons.org/licenses/by/4.0/>).

manifested as the decline of quality in the grassland ecosystem (including vegetation and soil), productivity, economic potential and ecosystem services, the deterioration in ecological environment, and the decrease in biodiversity and landscape complexity, whilst recovery functions are weak or lost completely (Wang, 2004). China is the second-largest steppe country in the world, and natural grassland accounts for 40% of the country's total area of land. In recent decades, China's grasslands have experienced large-scale desertification, degradation, and salinization, which form an important source of sandstorms.

Grassland degradation is a major issue related to the sustainable development of the social economy (Li, 1997). At present, the monitoring of grassland degradation mainly includes field observation and inspection methods (Gu et al., 2010; Wang et al., 2004; Xue et al., 2009) and remotely sensed methods (An et al., 2017, 2014; Chen et al., 2010; Gardiner et al., 2016; Li, 1997; Nicholson et al., 1998; Wang et al., 2014; Zhang et al., 2017a; Zhao, 2012). The former type of methods is accurate, but they are labor-intensive and time-consuming, and subject to local experience and expertise. The indicators of grassland degradation mainly include biological indicators (e.g. vegetation coverage, biomass, dominant species, etc.) and soil traits (Yan, 2008). Soil traits are extremely difficult to obtain at regional scales, whereas biological indicators are often used to evaluate large-scale grassland degradation. Remote sensing methods can provide information on the vegetation coverage, biomass, etc. at large regional scales. Therefore, changes in vegetation coverage or biomass information derived from remotely sensed imagery are often used to evaluate grassland changes (An et al., 2017; Bastin et al., 2012; de Jong et al., 2011; Eddy et al., 2017; Fensholt et al., 2012; Geerken and Ilaoui, 2004; Karnieli et al., 2013; Li et al., 2012; Liu et al., 2008; Meroni et al., 2017; Eckert et al., 2015). With the increasing use of remotely sensed imagery and products such as AVHRR, MODIS and SPOT VEGETATION (de Jong et al., 2011; Li et al., 2020b), more attention has been paid to characterize the changes of grassland productivity through trend analysis of long-term sequence vegetation indices (such as the Normalized Difference Vegetation Index (NDVI) as a proxy for the net primary productivity (NPP) or above-ground biomass) (Bai et al., 2008; Fensholt et al., 2012; Shen et al., 2018). However, these methods do not take into account reducing the effects of climate fluctuations on grassland productivity over the years and may not be able to reflect the real grassland condition. In addition to human activity, the vegetation status and growth rates are also dependent on the climatic conditions affected by water availability and thermal conditions. Regional climates have certain fluctuations and periodicity. The periodic climatic factors (such as precipitation, temperature, etc.) will cause "poverty years" and "abundant years" of grassland plant growth across different years. The annual changes in the grassland biomass might be the results of climate fluctuations or grassland degradation. Similarly, the grassland biomass could be used as a proxy indicator to evaluate grassland degradation, and the impact of climate fluctuations need to be considered to better understand grassland changes. Researchers have previously adopted the rainfall use efficiency (RUE) (Brown de Colstoun et al., 1998; Gao et al., 2005; Holm et al., 2003) and energy use efficiency (EUE) to reduce the impacts of climate fluctuations (Bai et al., 2008; Brown de Colstoun et al., 1998; Houerou and Henri, 1984), with the applications on grassland degradation areas. In addition, there are other methods developed for monitoring grassland degradation by considering climate impacts include LNS (Local NPP Scaling) (An et al., 2017; Prince, 2012; Prince et al., 2009; Wessels et al., 2008), and time-series analysis using nonlinear seasonal-trend analysis (Prince, 2012; Eckert et al., 2015; Shen et al., 2018), the residual trend analysis method derived from the RUE (Burrell et al., 2017; Cai et al., 2015; Evans and Geerken, 2004; Leroux et al., 2017; Li et al., 2012; Wessels et al., 2007; Xu et al., 2010) and the simulation of the potential NPP through global vegetation physiological and biochemical models such as the Lund-Potsdam-Jena dynamic vegetation model (LPJ) (Seaquist et al., 2008; Zika and Erb, 2009).

The processes and causes of grassland degradation have received

significant attention (Zhang et al., 2017b), and the research on grassland degradation is still in its infancy due to the complexity (Yan, 2008). Both equilibrium and non-equilibrium models were adopted to unravel the mechanism of grassland vegetation succession (Vetter, 2005). The equilibrium model highlights the importance of biotic feedback such as the density-dependent regulation of livestock populations and the feedback on livestock density with respect to vegetation composition, cover and productivity. In contrast, non-equilibrium rangeland systems are thought to be driven primarily by stochastic abiotic factors, notably, variable rainfall, which results in highly variable and unpredictable primary production. Recent studies suggest that most arid and semi-arid rangeland systems encompass elements of both equilibrium and non-equilibrium at different scales. Therefore, the monitoring of spatial-temporal patterns of large-scale grassland degradation is still lack of an effective and generalized method.

This research focuses on the three river headwater region (TRHR), which is the birthplace of three major rivers, the Yangtze, Yellow and Lancang Rivers, is located in the hinterland of the Qinghai-Tibet Plateau. It is an international research hotspot and has a vast area with a harsh natural environment of high altitude, thin air, and a dry and cold climate. This has brought challenges in data acquisition and field-based research, and caused differences in the understanding of degraded grassland areas, spatial distribution characteristics, and degeneration causes in the area (An et al., 2017; Harris, 2010; Liu et al., 2008; Verón et al., 2006; Wu et al., 2014; Zhang et al., 2017; Li et al., 2020).

In recent years, researchers have made pioneering explorations on grassland dynamics in the study area. Different methods, data and indicators have been developed and applied for remotely sensed monitoring of grassland changes. For example, grassland change information was derived by comparing multi-period grassland status data based on visual interpretation and human-computer interaction (Liu et al., 2008); Different ecological units or production capacity units were divided for grassland according to natural conditions, and un-degraded reference values was identified at the same unit, and such indicator was adopted to quantify the grassland degradation (Wu et al., 2014; An et al., 2017); DBEST (Detecting Breakpoints and Estimating Segments) was applied for trend analysis of NDVI time series, such that vegetation change was detected and the impact of ecological conservation was demonstrated (Shen et al., 2018); The combination of vegetation coverage and spatial heterogeneity indicators was used to identify grassland conditions and monitor changes in grassland (Li et al., 2020a). Vegetation dynamics and its driving factors in the study area from 1982 to 2012 have been explored, where the dominant factors for grassland changes are distinct over different periods. The major remote sensing data sources used are NOAA / AVHRR-NDVI, MODIS-NDVI, and Landsat series imagery. The indicators used for monitoring involve NDVI, NPP, vegetation coverage, spatial heterogeneity, etc.

In this research, we comprehensively considered multiple meteorological factors and constructed a novel ecosystem characteristic index suitable for the climatic characteristics of TRHR to monitor grassland dynamics by combining remote sensing and time-series climate data. The main scientific contribution of this paper are as follows: (1) Propose a Novel Rainfall Use Efficiency index (NCUE) for monitoring grassland dynamic which is suitable for cold and arid climate characteristics of the Qinghai-Tibet Plateau to reduce the effect of inter-annual variability of grassland productivity caused by climate fluctuation; (2) Construct an Integrated Meteorological Factor (IMF) based on the analysis of dominant climatic elements affecting vegetation growth; (3) Reveal the spatial temporal characteristics of grassland change from 1982 to 2012 in the TRHR by trend analysis of NCUE time series. A new understanding of the grassland dynamics in the study area was gained. In addition to the rainfall factor that affects the growth of vegetation derived in RUE, our proposed novel NCUE also considers the effects of temperature, land surface temperature, wind speed, sunlight, as well as time lag to build an integrated meteorological index IMF. Such NCUE is suitable for the "cold and dry" characteristics of the study area and has the ability to reduce

the impact of integrated climate fluctuations and detect grassland degradation objectively.

## 2. Study area and data source

### 2.1. Study area

The TRHR is located in the southern part of Qinghai Province at 31°39' to 36°12' north latitude and 89°45' to 102°23' east longitude. The whole area covers approximately 360 000 km<sup>2</sup>, and it includes 16 counties of Yushu, Guoluo, Hainan and Huangnan, and the Tanggula township of Golmud City (Fig. 1). The Tanggula township appears as Geermu in Fig. 1. The elevations range between 2800 m and 6564 m. The main mountain ranges in TRHR are the East Kunlun Mountains and their branch veins, the Animaqing Mountain, Bayankara Mountain and Tanggula Mountain Range. There are numerous rivers and lakes, and swamps are widely distributed across the area. The vegetation types are predominantly alpine meadows and alpine grasslands. The area has the highest concentration of biodiversity in high-altitude regions in the world. The originality and vulnerability of the vegetation are well documented (Liu et al., 2005). The climate of the TRHR belongs to the Qinghai-Tibet Plateau climate system, and it is a typical continental climate at high altitude (Li et al., 2006). TRHR is characterized by alternating hot and cold seasons, small annual temperature differences, large daily temperature differences, long sunshine duration, and strong radiation, and the distinction among four seasons is not obvious throughout the year.

The nature reserves in TRHR are currently the largest in China. The nature reserves are divided into 6 regions and contain 18 protected sub-areas, with a total area of 152000 km<sup>2</sup>, accounting for 42% of the total area of the TRHR. The distributions of the research area, nature reserves, field observation sites and weather stations are shown in Fig. 1.

### 2.2. Data source

The NDVI data used in this research are NOAA/AVHRR-NDVI data from 1982 to 2001 and Terra/MODIS-NDVI (MOD13) data from 2000 to 2012. The AVHRR-NDVI data are from the Pathfinder AVHRR NDVI, which is freely available from the China Western National Environmental and Ecological Scientific Data Centre (<http://westdc.westgis.ac.cn>). The dataset has a temporal resolution of 10 days and a spatial resolution of 8 km × 8 km. The 16-day Terra/MODIS-NDVI data with a spatial resolution of 250 m was obtained from the NASA (<https://modis.gsfc.nasa.gov/>).

The daily meteorological data from 36 weather stations in the study area and its surrounding areas were acquired from 1982 to 2012. At the

same time, a high-precision 0.5° × 0.5° grid data set (V2.0) was used, including daily rainfall value, monthly value, daily surface temperature, and monthly value of the ground surface in China. The data was downloaded from China Meteorological Data Service Centre (<http://data.cma.cn>). The China Regional Surface Meteorological Elements data set (ITPCAS) (He et al., 2020) and grid data set of CRU TS 3.21 with spatial resolution of 0.5° × 0.5° were also adopted (Huang et al., 2013).

The land use/cover (LULC) data at a scale of 1:100,000 was downloaded from the Chinese Academy of Sciences Resource and Environmental Science Data Center, covering the temporal range from the 1980 s, 1990, 1995, 2000, 2005 and 2010 (<http://www.resdc.cn>). Visual image interpretation was employed to identify LULC types using the Landsat TM/ETM + satellite images at the corresponding dates. These LULC data were classified into six primary types initially, which were cultivated land, woodland, grassland, water bodies, residential areas and unused areas. Then, twenty-five secondary types were further classified. Cultivated land refers to paddy fields and dry croplands. Woodland refers to woodland, shrubbery, sparse woodland and other wooded lands. Grassland refers to high-coverage grassland, medium-coverage grassland and low-coverage grassland. Water bodies include rivers, canals, lakes, reservoirs, pits, glaciers, permanent snow, tidal flats and beaches. Residential areas refer to residential land in urban, rural, industrial and mining areas. Unused areas contain sand, Gobi, saline-alkali, marsh, bare land, bare rocky gravel and other unused land types. Bare land in the unused areas refers to a large area of bare land with almost no grass distributed in it. Bare soil contained in degraded pastures is not included in the unused areas. Usually, grass and bare soil are mixed in degraded pastures. The LULC data was used for comparative analysis of the detected grassland change results.

From August 11 to 21 in 2013, a comprehensive field survey and spectral measurements were conducted in the study area. The route and the selection of the quadrat locations (Fig. 1) were designed based on satellite imagery, Google Maps, road and river distribution maps, topographic maps, LULC maps and grassland resource maps. The sampling sites were chosen on both sides of roads where the terrain was flat and open, and the degree of grassland degradation was relatively uniform. They were sparsely distributed and were at least 2 km apart from each other. The spectra of various grass species, bare soil, water bodies, and various degrees of degraded grassland were measured extensively.

The sample area is 30 × 30 m<sup>2</sup>. GPS determined the center position of the sample. Using the "X" sampling method (Fig. 2), five sampling points were placed within each large sample, and a 0.5 × 0.5 m<sup>2</sup> sample box was placed at each sampling point. Expert knowledge was used to visually estimate the vegetation coverage, including the total coverage and component coverage of various grass species within the 0.5 × 0.5 m<sup>2</sup>

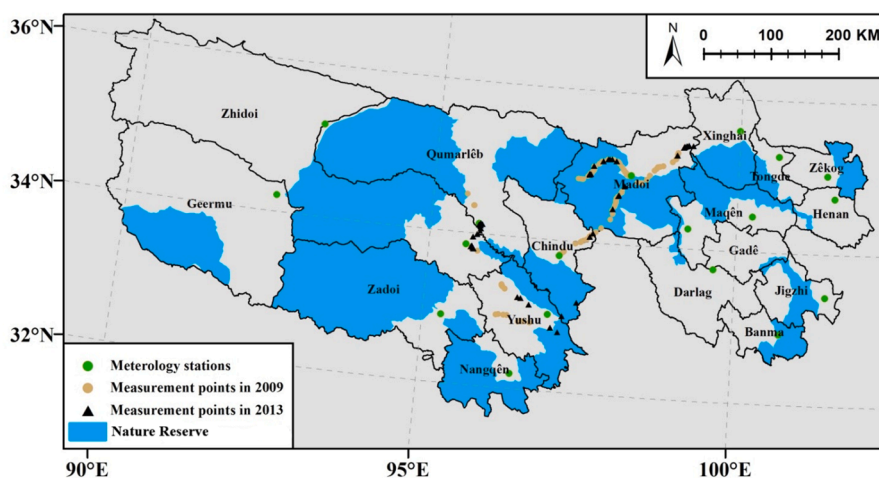
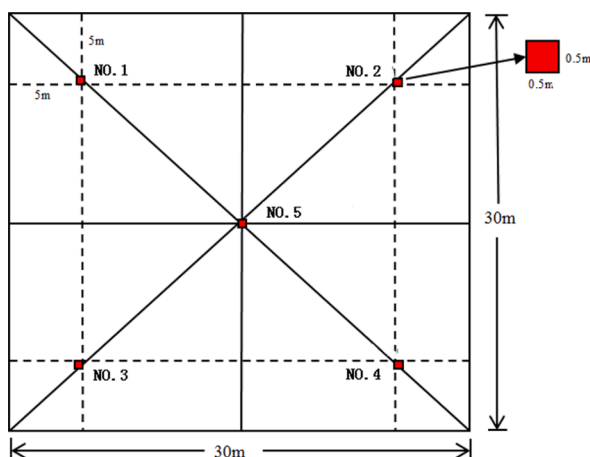


Fig. 1. Distributions of research areas, nature reserves, filed observation sites and weather stations.



(a)



(b)

Fig. 2. The sketch of the sampling spots: (a)  $30 \times 30 \text{ m}^2$  large quadrat; (b)  $0.5 \times 0.5 \text{ m}^2$  small quadrat.

sample boxes. An error of  $<5\%$  was achieved when compared with the results identified from photographs taken in the field. The  $30 \times 30 \text{ m}^2$  large square coverage was obtained based on the average coverage of five small squares. At the same time, photographs and records at the location of each sample site, along with weather conditions and geographical features were collected comprehensively (Fig. 3). A total of 56  $30 \times 30 \text{ m}^2$  quadrats were obtained for the delineation of the grassland degradation level. These were used for comparative analysis of the grassland changes derived in the research. Moreover, the administrative boundary vector maps, nature reserve vector map, DEM data with a 100-meter resolution, and a Qinghai Province 1: 1,000,000 grassland type distribution map of the TRHR were used. The DEM data was used for meteorological data interpolation, and the grassland type distribution map was used for extracting grassland information.

In August 2009, a comprehensive field survey was also conducted. Based on the experience of experts, the grassland situation of 70 inspection sites was recorded. This information will also be used for comparative analysis of the results of this article.

### 3. Methods

There are six main research steps in this paper, including data collection, data preprocessing, IMF construction, NCUE establishment and grassland changes monitoring, analyzing the spatiotemporal characteristics of grassland changes, and analyzing and discussing the results. Detailed descriptions of the methodology are presented in the following sections.

#### 3.1. Data preprocessing

##### 3.1.1. Preprocessing remotely sensed data

The preprocessing step included projection transformation, monthly maximum NDVI synthesis, and scale transformation. Both NOAA/AVHRR-NDVI and MODIS-NDVI (MOD13) were projected onto the Albers Conical Equal Area. NDVI composites were created using the maximum value composite (MVC) technique (Holben, 1986), using the highest AVHRR-NDVI from daily images over 10-day periods. The MODIS-NDVI from daily images over 16-day periods was selected as the least affected by clouds or the atmosphere. Correlation analysis of the overlapping period of the two different NDVI data in 2000–2001 was carried out, and a linear regression model was fitted to modify the differences of the NDVI between two different sensors (Lu, 2011). The estimated NOAA  $8 \text{ km} \times 8 \text{ km}$ /AVHRR NDVI was resampled to a 250-m spatial resolution to be consistent with that of MODIS-NDVI. The NDVI values for each month of the growing season were accumulated to obtain the cumulative NDVI ( $\sum \text{NDVI}$ ) in the growing season.

After analyzing the meteorological station-measured temperature data, it was found that from May 8 to September 28, the temperature was stable at  $0^\circ \text{C}$  or above during the majority of years, so this period was regarded as the growing season. In this case, the growing season lasts from May to September (Lu, 2011).

##### 3.1.2. Spatialization of climatic elements using multiple data sources and multiple methods

First, a cumulative treatment was applied to the rainfall at the



(a)



(b)

Fig. 3. Typical extremely degraded grassland landscape: (a) Iron bar hammer – a typical degraded grass species, at Zarlina Lake; (b) “Black Earth Beach” rodent.

monthly scale and the scale of growing seasons. Mean values were used for temperature, sunshine duration, wind speed, and surface temperature. Meteorological stations in the TRHR are scarce, especially in the west, which affects the accuracy of interpolation. The spatial resolution of existing grid data is  $0.5^\circ \times 0.5^\circ$  (i.e., an average spatial resolution of 49.0 km for longitude and 55.6 km for latitude), which does not match the spatial resolution of MODIS NDVI at 250 m. According to Gao et al. (2014), we used the data of the grid cell center (derived from grid data sets) and weather stations to perform further interpolation to obtain grid data with a spatial resolution of 250 m. GRADS 2.0 was used to generate the corresponding grid center point data. These grid center points were used as supplemental sites, and then ArcGIS Geostatistics software was used for interpolation. For many spatial interpolation methods for meteorological data, there is no optimal interpolation method suitable for all meteorological elements. After analysis and comparison, rainfall and sunshine hours were rasterized using Geostatistics Ordinary Kriging (OK), and cross-validation showed that the accuracy was over 90%. The temperature and land surface temperature were rasterized using multiple regressions and residual OK methods with an accuracy of 90%. The wind speed was rasterized using topographic factor correction (Fu, 1983; Lu et al., 2009), and the accuracy was over 85%. The interpolation results could meet the research requirements of this paper.

### 3.2. Integrated meteorological factor (IMF) construction

The growth of grassland vegetation is mainly affected by the climate, soil, grass species characteristics itself, and human activities. For a certain region, changes in the soil properties and grass species composition are relatively stable over a specific time scale, while the climatic factors fluctuate significantly each year, which may lead to annual changes in grassland vegetation. Sunlight, temperature and precipitation are the basic climatic factors affecting vegetation growth (Gu et al., 2010; Lu, 2011; Qian et al., 2010, 2007; Yu, 2013). The TRHR has cold climatic conditions and the existence of frozen soil has great impacts on the grassland vegetation growth (Xue et al., 2009). The surface temperature is an important factor affecting the frozen soil. Precipitation is also a limiting factor of vegetation growth in the study area (Wang et al., 2014). In addition, the strong wind speed and its variation in the region will affect the regional evaporation and soil moisture. As a consequence, vegetation growth is also influenced (Gardiner et al., 2016; Zhao, 2012). The response of grassland vegetation to the climate has lag effects (An et al., 2014; Zhang et al., 2017a), and different regions and vegetation types have different responses to the climate (Chen et al., 2010). Therefore, the main climatic factors were chosen as the temperature, precipitation, sunshine, surface temperature, wind speed, and lag effects.

Using data from thirteen meteorological sites and the Pearson correlation analysis, the relationship between  $\sum$  NDVI and each climatic factor was established for each year. Then, take the 31-year average as the multi-year average correlation coefficient. It was found that  $\sum$  NDVI has a good correlation with each climatic factor, and all passed the  $p < 0.01$  significance test. Five climatic factors in the growing season were chosen as the main climate impact factors.

The time lag responses of  $\sum$  NDVI to the five types of climatic factors in the region are different. For the temperature, the correlation between  $\sum$  NDVI and the temperature in April of each year is the highest, of which the lag period of  $\sum$  NDVI to the temperature response maybe one month. For the wind speed, the highest correlation appears in March, and the lag period maybe approximately two months. For the surface temperature, the highest correlation appears in February, and the lag period maybe three months. For precipitation and sunshine hours, the correlations reach the maximum during the growing season, and the lag period maybe less than one month. Thus, the three factors of the average temperature in April, the average wind speed in March, and the average surface temperature in February were selected as the major time-delay factors. The correlation analysis of

the cumulative NDVI in the growing season and the effects of the time lag of various climatic factors are listed in Table 1. An annual accumulated temperature of greater than  $0^\circ\text{C}$  is used to characterize the heat demand for vegetation growth and development (He et al., 2020), which was also selected as one of the major climate impact factors.

In addition, evaluations of the local appropriate degree of rainfall, temperature and sunshine for grassland vegetation growth were conducted. All the suitability values of every 10 days during the growing season were derived by adding them together. They were named as the rainfall condition index, temperature condition index and sunshine condition index, respectively, and chosen as three key indices.

Taking the water conditions of a particular 10 days as an example, the suitability value is computed as follows (Qian et al., 2007):

When the precipitation reaches the perennial average of 10 days, this indicates that the water supply meets the normal standard for grassland vegetation adaptation. At this time, the water condition index is assumed to be 1. Precipitation of  $<50\%$  during the normal period is regarded as the limit of the lack of precipitation (drought). The rainfall suitability model for 10 days is derived as:

$$I_p = \begin{cases} 1 & p \geq \bar{p} \\ \frac{1}{1 + ((\bar{p} - p)/p_m)^2} & 0 \leq p < \bar{p} \end{cases} \quad (1)$$

$$p_m = 0.5\bar{p} \quad (2)$$

Where  $I_p$  is the rainfall suitability value for 10 days.  $P$  is the precipitation during this 10-days valuation period.  $\bar{p}$  is the perennial average value during the evaluation period.  $p_m$  is the lower bound of precipitation values, please refer to Qian et al. (2007). Precipitation, temperature and sunshine are mutually restricted and interacting with each other. If these three elements are matched and coordinated, the overall meteorological conditions will be conducive to the growth of grassland vegetation, but if anyone element deviates, it will limit the play of the other elements. According to this principle, the light, temperature and water matching index (STPC) (Huang et al., 2013; Lu, 2011; Qian et al., 2007; Yang, 2012) was constructed and selected. The index takes the minimum of the three conditional indices of the growing season, which is also referred to as the principle of minimum restriction (Qian et al., 2007).

Based on these selected climate factors, an integrated meteorological factor (IMF) index is established to capture the multiple linear relationships. The IMF is expressed as:

$$IMF = a_1X_1 + a_2X_2 + a_3X_3 + \dots + a_nX_n \quad (3)$$

Where  $X_1, X_2, X_3, \dots, X_n$  are meteorological factors that affect the vegetation NDVI,  $a_1, a_2, a_3, \dots, a_n$  are the weight coefficients of each factor, and  $n$  is the number of selected meteorological factors. In this paper,  $n$  is 13. The IMF characterizes both climatic contributions to the NDVI, and also reflects the comprehensive meteorological conditions affecting the vegetation growth.

Using the yearly  $\sum$  NDVI as the dependent variable and corresponding climatic factors as independent variables, then, we can establish an equation set of 31 equations and a linear equation was fit on a per-pixel level by regression analysis using ordinary least-squares or partial-least-squares and the contribution weight of each climatic factor would be achieved as a pixel-wise IMF estimation. The specific climate factor values of a certain year were brought into eq. (3), and integrated meteorological factor can be obtained for each pixel of each year.

### 3.3. The grassland ecosystem characteristics index (NCUE) and grassland changes monitoring

#### 3.3.1. Establishing the NCUE

The rainfall use efficiency (RUE) is defined as the ratio between the

**Table 1**

Correlation between the cumulative NDVI during the growing season and the climatic factors of each month before the growing season.

	Average temperature	Cumulative rainfall	Average sunshine hours	Average wind speed	Average surface temperature
January	0.490**	0.755**	-0.557*	-0.780**	0.514**
February	0.518**	0.838**	-0.575*	-0.781**	0.536**
MarchApril	0.524**0.530**	0.869**0.860**	-0.641*-0.717**	-0.810**-0.806**	0.388**0.429**
Growing season	0.418**	0.889**	-0.824**	-0.788**	0.511**

(\*:  $p < 0.01$ ; \*\*:  $p < 0.001$ )

annual aboveground primary production and the annual precipitation. It can be calculated from remotely sensed biomass (such as the NDVI) and precipitation data. The TRHR has the characteristics of “cold and dry”, and precipitation is not the single climatic factor that affects the growth of grassland vegetation. Thermal conditions play an important role in the growth of grassland vegetation. Similar to the RUE, the IMF, which is composed of multiple climatic factors affecting vegetation growth, was introduced into NCUE model, and a grassland ecosystem characteristic index (NCUE) suitable for the climatic characteristics of the study area was established:

$$NCUE = \frac{\sum NDVI}{IMF} \quad (4)$$

Where NCUE is the grassland ecosystem characteristics index,  $\sum NDVI$  is the NDVI accumulation of the growing season, and IMF is the integrated meteorological factor. If the NCUE declines over time, the conditions of the grassland may become worse. If the NCUE is on the rise over time, this means that the grasslands might be improved. If the trend of the NCUE is unchanged, this indicates that the grassland status may remain unchanged. In this study,  $\sum NDVI$  was chosen as the proxy indicator of the annual vegetation biomass of grassland (Stow et al., 2004; Sun, 2015).

### 3.3.2. Trend analysis of the NCUE to monitor grassland changes

A trend analysis of NCUE time-series data from 1982 to 2012 was performed to determine the changes of grassland at the pixel level. This established a linear regression over time. The slope and correlation coefficient of the regression equation were calculated, and the correlation coefficient was tested statistically at a 95% confidence interval. A negative slope value defines degradation and a positive value reflects recovery. The greater the absolute value of the slope, the higher the degree of grassland degradation or restoration. The significance of time-series trends is used to characterize changes in grasslands, such as significant degradation, degradation, recovery and significant recovery. Significant degradation describes an area that has a negative slope and passes the 95% confidence interval, while degradation (but not significant) refers to the areas that have a negative slope but do not pass the significant test. Recovery (but not significant) refers to areas with positive slopes but do not pass the significant test. Significant recovery refers to areas with significantly positive slopes at a 95% confidence interval. Unchanged refers to areas with a slope of  $-0.0017 \sim 0.0013$  (these thresholds were determined based on the field observation and LULC data).

### 3.4. Comparing and analyzing the rangeland changes

The field observed data acquired in 2013 and 2009, land use/cover change maps and the change trend of accumulated NDVI in the growing season were used to compare and analyze the monitoring results of grassland degeneration. According to Pan (2007), a two-steps cluster is employed based on the analysis of grassland conditions, division standard and the study area situation. The input data is the native plant species, poisonous weeds, and bare soil component with coverage of sample plots. The grading standards of the grassland status were obtained thereafter. The grassland status was classified into five categories of non-degradation, mild degradation, moderate degradation, severe

degradation and extreme degradation (Pan, 2007; Yu et al., 2012) (Table 2). The changing trend of the NCUE from 1982 to 2012 is different from the grassland degradation situation according to their definitions. Although the former is the changing trend and the latter is the change outcome, these two might have some connections.

## 4. Experimental results and analysis

### 4.1. Changing trend of accumulated NDVI during the growing season, the IMF and NCUE

Changing trend from 1982 to 2012 for accumulated NDVI during the growing season is shown in Fig. 4. It indicates that from 1982 to 2012, the NDVI in TRHR showing an overall increase trend. The percentage of significantly increased NDVI is 42.17%, which cover the largest area of the TRHR, while the percentage of insignificantly increased is 13.52%; the percentage of significantly decreased NDVI from 1982 to 2012 is 31.90%, cover the secondary largest area of the TRHR, and the percentage of insignificantly decreased NDVI is 12.41%.

The significantly increased NDVI mostly distributed in southeast and south center of the TRHR, such as Zêkog, Henan, Jigzhi, Banma, Darlag, south and center part of Xinghai, Yushu, Nangqên, Zadoi, Cindu and the south part of the Zhidoi, while the insignificantly increased NDVI mostly distributed in west part of the TRHR, such as Geermu and the north part of Zhidoi. The significantly decreased NDVI were mostly distributed in the north and center part of the TRHR, such as the most part of Madoi, east and west part of Qumarlêb that adjacent to Madoi and Zhidoi, center and north part of Zhidoi, east and northeast part of Geermu that adjacent to Zhidoi.

Change trend from 1982 to 2012 for the IMF is shown in Fig. 5. It shows that from 1982 to 2012 the IMF in TRHR showing an overall increase trend. The percentage of significantly increased IMF is 45.07%, which cover the largest area of the TRHR, while the percentage of insignificantly increased is 10.67%; the percentage of significantly decreased IMF from 1982 to 2012 is 34.34%, cover the secondary largest area of the TRHR, and the percentage of insignificantly decreased IMF is 9.92%.

The IMF in the TRHR shows a trend of decreasing gradually from southeast to northwest. The meteorological conditions in the northwest were relatively poor, and the vegetation growth was relatively poor. Areas where the cumulative NDVI and climatic factors have established an effective model account for 75.65% ( $P < 0.01$ ), and 91.427% ( $P < 0.05$ ) of the total area of grassland. This indicates that apart from the meteorological elements listed in this article, human activities could

**Table 2**

Degradation degree judgment matrix of alpine meadow grassland.

Degradation level	Native plant species ratio(%)	Poisonous weeds ratio(%)	Bare soil ratio(%)
Non-degradation	$\geq 72$	$\leq 15$	$\leq 10$
Mild degradation	55–72	15–35	10–25
Moderate degradation	35–55	35–50	25–50
Severe degradation	20–35	50–75	45–80
Extreme degradation	$\leq 20$	$\geq 75$	$\geq 80$

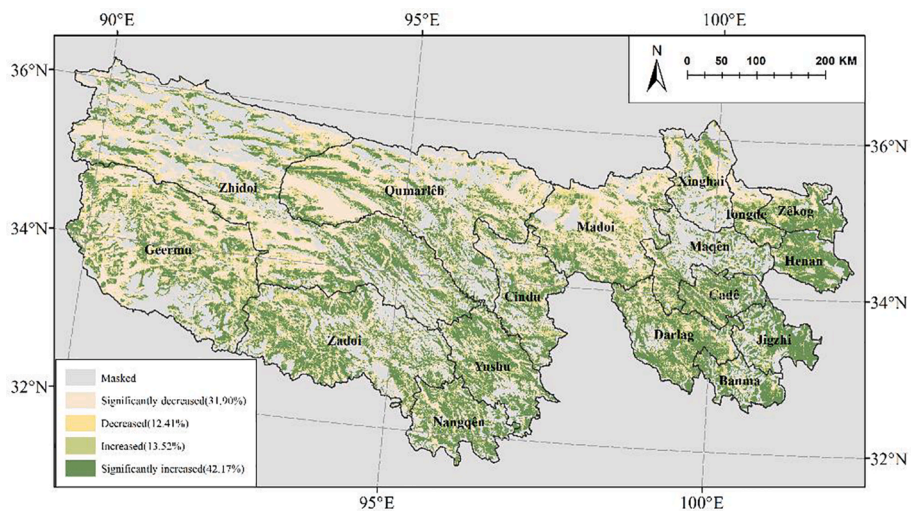


Fig.4. Change trend from 1982 to 2012 for accumulated NDVI during the growing season.

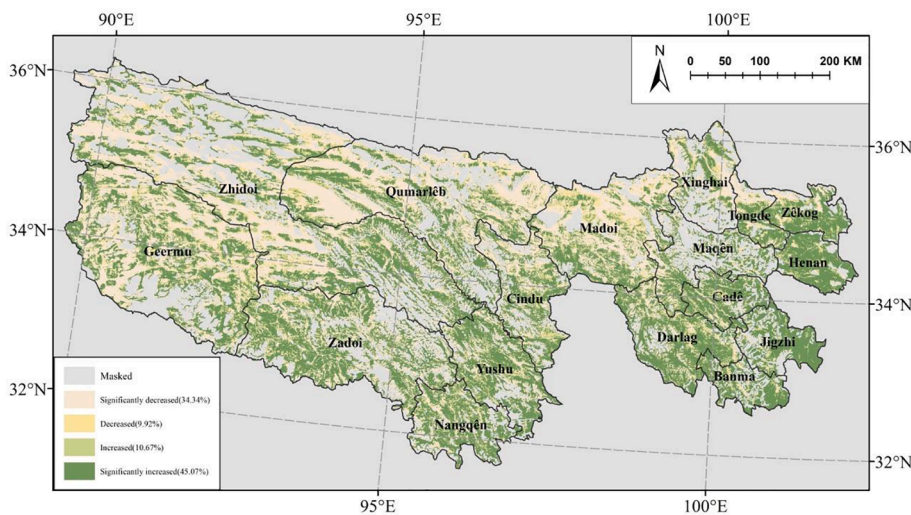


Fig.5. Change trend from 1982 to 2012 for the IMF.

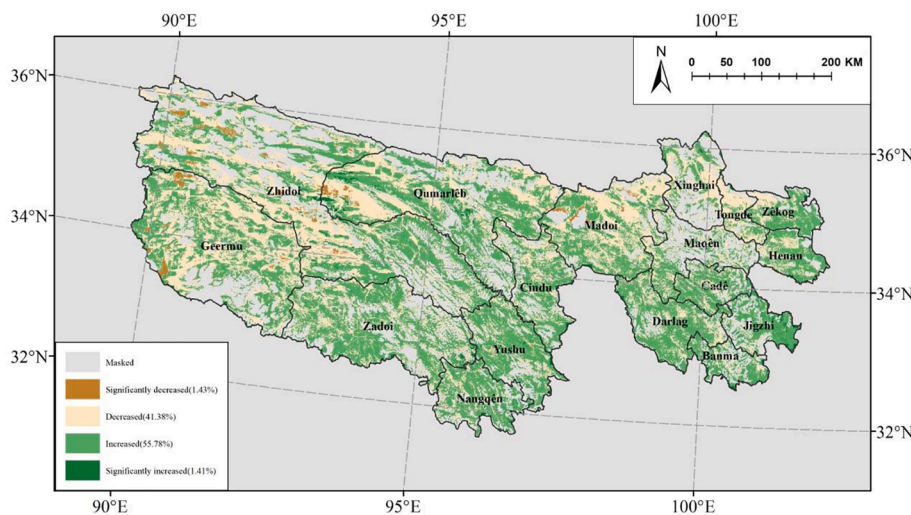


Fig.6. Change trend from 1982 to 2012 for the NCUE.

have an impact on the growth of grassland vegetation in these areas. In the study area, the time series mean of the accumulated NDVI showed inter-annual fluctuations from 1982 to 2012 during the growing season. Overall, NDVI presents a situation where increasing and decreasing coexist. The IMF showed a similar changing characteristic. The change trends of the accumulated NDVI and IMF are similar in large spatial patterns, illustrating that the climate factors contribute a large part to the NDVI change in the TRHR. But there are differences between them in local areas (Please look carefully at Fig. 4 and Fig. 5). In addition, the area ratio of each change level is also different.

Change trend from 1982 to 2012 for the NCUE is shown in Fig. 6. It indicates that from 1982 to 2012 the NCUE in TRHR showing an overall increase trend. The percentage of significantly increased NCUE is 1.41%, which cover the smallest area of the TRHR, while the percentage of insignificantly increased is 55.78%. The percentage of significantly decreased NCUE from 1982 to 2012 is 1.43%, which also covers the smallest area of the TRHR; the percentage of insignificantly decreased NCUE is 41.38%, which is the second largest proportion. The spatial distribution pattern for NCUE is similar to that of NDVI and IMF.

#### 4.2. Spatial distribution characteristics of grassland degradation and restoration

The spatial distribution of grassland changes from 1982 to 2012 determined by the temporal trends of NCUE is shown in Fig. 7. In this figure, the degraded grassland in the study area accounted for 20.49% of the total area of grassland. Among these areas, significant degradation accounts for 1.43% ( $P < 0.05$ ), and degradation but not significant accounts for 19.06%. Grassland restoration accounts for 23.49% of the total grassland area. Significant recovery accounts for 1.41%, and recovery but not significant accounts for 22.08%. Grassland basically unchanged area accounts for 56.02% of the total grassland area.

The above trend analysis shows that in the past 31 years, the status of the grassland in TRHR has improved. Grassland ecosystems in some areas show a recovery trend, but there are still some areas that continue to deteriorate. The spatial distribution includes: (1) In Central Yushu County and Nangqên County, a large area of grassland restoration appears. Towards Cindu County, Qumarlêb County and Zadoi County, the grassland restoration also happens; (2) the southeast of Jigzhi County, south of Darlag County, Xinghai county recovery is significant; (3) Grassland degradation was mainly distributed in the northeast of Maduo County, west of Qumarlêb and Zhidoi County, as well as the Geermu local area. Grassland restoration also exists in these areas.

#### 4.3. Comparison and analysis of grassland degradation and restoration results

The results achieved in this paper are compared and analyzed with LUCC, trend of the accumulated NDVI during the growing season, and field observation data obtained in 2013 (56 samples) and 2009 (70 samples), as shown in Table 3 and Table 4. From the tables, we can see that: (1) areas with negative NCUE slopes usually correspond to grassland with different degrees of degradation observed in the field and (2) the NCUE slope of the non-degenerated areas observed in the field is mostly positive. The ratio in both cases is about 68% (denoted by Y in Table 3 and Table 4). This shows that there might be some connections between the changing trends and field observed grassland degradation status.

For non-degraded grasslands observed in the field, there are three types of trends of the NCUE. One is positive, which means that the areas are restored from grasslands with different degrees of degradation or the areas with non-degraded grassland. The second type is remaining unchanged. The last is negative, such as the healthy grassland area that has undergone slight degradation but still belongs to an un-degraded level. Table 3 and Table 4 show that many sites belong to the first case.

Areas with positive or almost constantly changing trends are not necessarily the un-degraded grasslands, and they could be recovered from grasslands with different levels of degradation. For example, for point 21 (35.00939 N, 97.59611 E) in Table 3, the NCUE trend value is 0.005, indicating that the grassland was recovering during the 31 years, and the changing trend of the LULC also shows that from 1990 to 1995, the point changed from sandy land to moderately covered grassland, and there has been no change thereafter. The grassland at this point tends to recover. However, moderately degraded grasslands were observed in the field. The actual situation is that the area has recovered from extremely degraded sandy lands, rather than degraded from lightly degraded or un-degraded grasslands.

The monitoring results of this study were also compared and analyzed with the change trend of the LULC and the accumulated NDVI (See Table 5 for the results). Due to more than 70% of the NDVI change trend is a significant change, this paper does not define the level of unchanged grassland by using NDVI. Therefore, the points where the LULC is unchanged are not considered (such as points 1, 12, etc. with a gray background in Table 3). In addition, some points whose trends of LULC type changes cannot clearly judged (such as points 4, 20, etc. in bold, italic and underlined font) are also removed. In the end, the samples compared with LULC were 25 in 2013 and 39 in 2009. The samples compared with NDVI and field observation were 56 in 2013 and

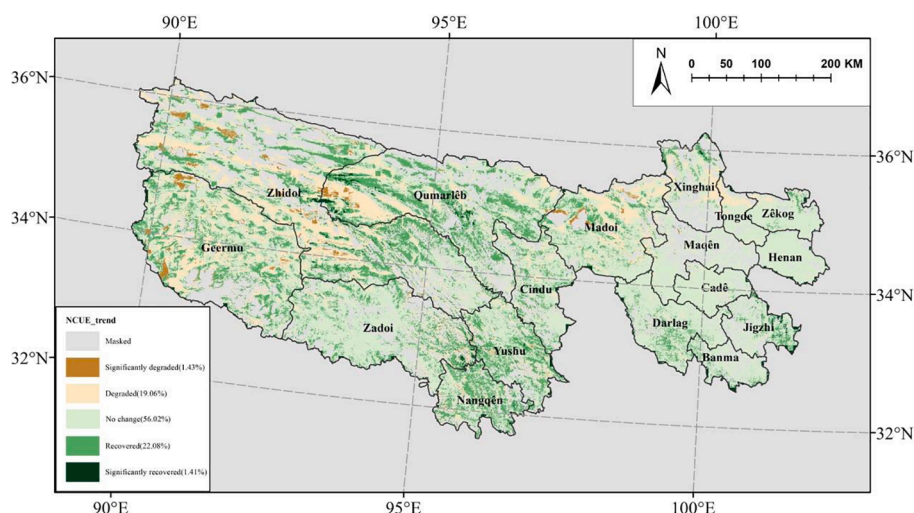


Fig. 7. Spatial distribution characteristic of grassland degradation and restoration from 1982 to 2012 by NCUE trend.

**Table 3**

Comparison of grassland changes detected by NCUE with field-observation data, LULC and NDVI change trend in 2013.

ID	Latitude	Longitude	FODS	A	B	C	D	E	NDVI_S	NCUE_S	R1	R2	R3	R4	R5
1	35.35564	99.21936	I	UC	UC	UC	UC	UC	-0.003841715	-0.001691300			Y		
2	35.35817	99.14418	II	UC	MC to BL	UC	UC	DE	-0.008705663	-0.010987038	Y	Y	Y	Y	Y
3	35.35122	99.11633	II	UC	BL to LC	UC	UC	RE	-0.009034017	-0.013418230	Y		Y	Y	
<b>4</b>	<b><u>35.34777</u></b>	<b><u>99.10384</u></b>	<b><u>II</u></b>	<b><u>LC to MC</u></b>	<b><u>MC to BL</u></b>	<b><u>UC</u></b>	<b><u>UC</u></b>	<b><u>UC</u></b>	<b><u>-0.008628733</u></b>	<b><u>-0.011451510</u></b>	<b><u>Y</u></b>	<b><u>Y</u></b>	<b><u>Y</u></b>	<b><u>Y</u></b>	<b><u>Y</u></b>
5	35.35819	99.14449	II	UC	MC to BL	UC	UC	DE	-0.007854215	-0.010987038	Y	Y	Y	Y	Y
6	35.35778	99.14461	III	UC	MC to BL	UC	UC	DE	-0.007854215	-0.008911362	Y	Y	Y	Y	Y
7	35.35569	99.14528	III	UC	MC to BL	UC	UC	DE	-0.00627514	-0.008911362	Y	Y	Y	Y	Y
8	35.35571	99.14529	III	UC	MC to BL	UC	UC	DE	-0.00627514	-0.008911362	Y	Y	Y	Y	Y
9	35.35563	99.14528	III	UC	MC to BL	UC	UC	DE	-0.00627514	-0.008812329	Y	Y	Y	Y	Y
10	35.35572	99.14535	III	UC	MC to BL	UC	UC	DE	-0.00627514	-0.008911362	Y	Y	Y	Y	Y
11	35.3559	99.14506	II	UC	MC to BL	UC	UC	DE	-0.00627514	-0.008911362	Y	Y	Y	Y	Y
12	35.33887	99.07852	II	UC	UC	UC	UC	UC	-0.009069584	-0.018127525	Y		Y	Y	
13	35.33831	99.07593	II	UC	UC	UC	UC	UC	-0.009252124	-0.009877190	Y		Y	Y	
14	35.33889	99.07623	III	UC	UC	UC	UC	UC	-0.009252124	-0.009877190	Y		Y	Y	
15	35.33104	99.06526	II	UC	UC	UC	UC	UC	-0.008830147	-0.015823964	Y		Y	Y	
16	35.11447	97.88955	II	UC	UC	UC	UC	UC	-0.004332194	-0.012704480	Y		Y	Y	
17	35.11191	97.84891	III	UC	MC to LC	UC	UC	DE	-0.001321627	0.0004284080				Y	Y
18	35.11121	97.82476	III	MC to LC	UC	UC	UC	DE	-0.001073083	-0.002376339	Y	Y	Y	Y	Y
19	35.11119	97.82474	II	MC to LC	UC	UC	UC	DE	-0.001073083	-0.002376339	Y	Y	Y	Y	Y
<b>20</b>	<b><u>35.08346</u></b>	<b><u>97.74453</u></b>	<b><u>II</u></b>	<b><u>UC</u></b>	<b><u>MC to Lake</u></b>	<b><u>UC</u></b>	<b><u>UC</u></b>	<b><u>UC</u></b>	<b><u>-0.000317136</u></b>	<b><u>0.0146827520</u></b>					Y
21	35.00939	97.59611	III	S to MC	UC	UC	UC	RE	-0.000360983	0.0050489130		Y		Y	
22	34.90438	97.53104	II	MC to LC	LC to S	UC	UC	DE	0.004509227	0.0130356370			Y		
23	34.90376	97.53127	II	MC to LC	UC	UC	UC	DE	0.004844830	0.0138548820			Y		
<b>24</b>	<b><u>34.90145</u></b>	<b><u>97.55336</u></b>	<b><u>II</u></b>	<b><u>LC to S</u></b>	<b><u>UC</u></b>	<b><u>UC</u></b>	<b><u>S to LC</u></b>	<b><u>0.000522814</u></b>	<b><u>-0.034139626</u></b>	<b><u>Y</u></b>					Y
25	34.89037	97.53186	II	UC	UC	UC	UC	RE	0.000201392	-0.044988625	Y				
26	35.0956	97.96458	II	UC	UC	UC	UC	UC	0.001784259	0.011186769			Y		
27	34.77374	98.125	I	LC to MC	UC	UC	UC	RE	0.004216325	0.032453351	Y	Y	Y	Y	Y
<b>28</b>	<b><u>34.64989</u></b>	<b><u>98.04014</u></b>	<b><u>I</u></b>	<b><u>LAKE to MC</u></b>	<b><u>MC to Lake</u></b>	<b><u>UC</u></b>	<b><u>UC</u></b>	<b><u>UC</u></b>	<b><u>0.001121222</u></b>	<b><u>0.017450565</u></b>	<b><u>Y</u></b>		<b><u>Y</u></b>	<b><u>Y</u></b>	<b><u>Y</u></b>
29	35.2203	98.96438	I	UC	LC to MC	UC	UC	RE	0.000573364	-0.007723934				Y	Y
30	34.63899	98.02946	I	UC	UC	UC	UC	UC	0.003921086	-0.031985901				Y	
31	34.46087	97.95137	III	UC	UC	UC	UC	UC	-0.007523185	-0.016297076	Y		Y	Y	
32	34.127	97.65768	I	LC to MC	UC	UC	UC	RE	-0.001505453	0.011327818		Y			
33	34.07806	97.61038	I	UC	UC	UC	UC	UC	0.005463828	0.009898725	Y		Y	Y	
34	33.20103	97.46926	II	UC	MC to LC	UC	UC	DE	-0.00019945	0.002483916				Y	Y
35	33.00867	97.24764	I	UC	BL to LC	UC	UC	RE	-0.012522309	-0.01971980					
36	32.79402	97.19837	II	HC to MC	UC	UC	UC	DE	0.006866030	-0.002596253	Y	Y			
37	32.84219	97.0757	II	UC	UC	UC	UC	UC	-0.002822498	-0.005253023	Y		Y	Y	
38	32.84219	97.0756	III	UC	UC	UC	UC	UC	-0.002822498	-0.005253023	Y		Y	Y	
39	33.12565	96.70239	II	UC	UC	UC	UC	UC	0.0013622580	0.000200635			Y		
<b>40</b>	<b><u>33.20386</u></b>	<b><u>96.56442</u></b>	<b><u>I</u></b>	<b><u>UC</u></b>	<b><u>MC to Lake</u></b>	<b><u>UC</u></b>	<b><u>UC</u></b>	<b><u>UC</u></b>	<b><u>0.002574169</u></b>	<b><u>0.004603553</u></b>	<b><u>Y</u></b>		<b><u>Y</u></b>	<b><u>Y</u></b>	<b><u>Y</u></b>
41	33.83283	95.69785	I	UC	UC	UC	UC	UC	-0.004609005	0.004329267	Y				
<b>42</b>	<b><u>33.82198</u></b>	<b><u>95.68428</u></b>	<b><u>II</u></b>	<b><u>LC to BL</u></b>	<b><u>BL to LC</u></b>	<b><u>UC</u></b>	<b><u>UC</u></b>	<b><u>UC</u></b>	<b><u>-0.000663235</u></b>	<b><u>0.015286485</u></b>					Y
<b>43</b>	<b><u>33.79259</u></b>	<b><u>95.72888</u></b>	<b><u>II</u></b>	<b><u>LC to MC</u></b>	<b><u>MC to LC</u></b>	<b><u>UC</u></b>	<b><u>UC</u></b>	<b><u>UC</u></b>	<b><u>0.004994782</u></b>	<b><u>0.004361200</u></b>				Y	
44	33.80899	95.71709	II	UC	UC	UC	UC	UC	0.002417488	0.042501174			Y		
45	33.80882	95.71704	II	UC	UC	UC	UC	UC	0.002417488	0.042501174			Y		
46	33.80893	95.71697	I	UC	UC	UC	UC	UC	0.002417488	0.042501174	Y		Y	Y	
47	33.95369	95.70775	II	UC	MC to LC	UC	UC	DE	-0.002750233	-0.011134764	Y	Y	Y	Y	Y
48	33.99134	95.7685	I	BL to MC	UC	UC	UC	RE	-0.006056834	0.008117074	Y	Y			
49	33.99133	95.76849	I	BL to MC	UC	UC	UC	RE	-0.006056834	0.008117074	Y	Y			
<b>50</b>	<b><u>34.01324</u></b>	<b><u>95.81013</u></b>	<b><u>II</u></b>	<b><u>MC to HC</u></b>	<b><u>HC to MC</u></b>	<b><u>UC</u></b>	<b><u>UC</u></b>	<b><u>UC</u></b>	<b><u>-0.004104727</u></b>	<b><u>-0.005211535</u></b>	<b><u>Y</u></b>		<b><u>Y</u></b>	<b><u>Y</u></b>	<b><u>Y</u></b>
<b>51</b>	<b><u>34.06713</u></b>	<b><u>95.8216</u></b>	<b><u>I</u></b>	<b><u>LC to HC</u></b>	<b><u>HC to LC</u></b>	<b><u>UC</u></b>	<b><u>UC</u></b>	<b><u>UC</u></b>	<b><u>0.003387089</u></b>	<b><u>-0.003873405</u></b>					
<b>52</b>	<b><u>34.10863</u></b>	<b><u>95.81035</u></b>	<b><u>I</u></b>	<b><u>MC to HC</u></b>	<b><u>HC to BL</u></b>	<b><u>BL to MC</u></b>	<b><u>UC</u></b>	<b><u>UC</u></b>	<b><u>-0.00202559</u></b>	<b><u>0.016639065</u></b>	<b><u>Y</u></b>				
<b>53</b>	<b><u>34.11975</u></b>	<b><u>95.78966</u></b>	<b><u>II</u></b>	<b><u>MC to HC</u></b>	<b><u>HC to MC</u></b>	<b><u>UC</u></b>	<b><u>UC</u></b>	<b><u>UC</u></b>	<b><u>-0.003015237</u></b>	<b><u>0.000939846</u></b>					
<b>54</b>	<b><u>34.11925</u></b>	<b><u>95.78921</u></b>	<b><u>I</u></b>	<b><u>MC to HC</u></b>	<b><u>HC to MC</u></b>	<b><u>UC</u></b>	<b><u>UC</u></b>	<b><u>UC</u></b>	<b><u>-0.000904993</u></b>	<b><u>0.000939846</u></b>	<b><u>Y</u></b>				
<b>55</b>	<b><u>034.13905</u></b>	<b><u>95.81607</u></b>	<b><u>II</u></b>	<b><u>BL to HC</u></b>	<b><u>HC to LC</u></b>	<b><u>UC</u></b>	<b><u>UC</u></b>	<b><u>UC</u></b>	<b><u>-0.011553417</u></b>	<b><u>-0.014404091</u></b>	<b><u>Y</u></b>		<b><u>Y</u></b>	<b><u>Y</u></b>	<b><u>Y</u></b>
<b>56</b>	<b><u>34.13008</u></b>	<b><u>95.84046</u></b>	<b><u>I</u></b>	<b><u>Non-grass</u></b>	<b><u>UC</u></b>	<b><u>UC</u></b>	<b><u>UC</u></b>	<b><u>UC</u></b>	<b><u>-0.003641036</u></b>	<b><u>-0.002743170</u></b>			<b><u>Y</u></b>		

(Here: Y means match; FODS: Field observed degradation situation; NCUE\_S: Slope of NCUE; NDVI\_S: Slope of NDVI; I means not degenerate; II means mildly degenerate; III means moderately degenerate; UC means essentially constant or unchanging; DE means degradation; RE means recover; BL means bare land; LC means lower coverage; MC means moderate coverage; S means sand; HC means high coverage; WL means wetland; BF means bush forest; and S to MC means sand land that has been turned to moderate coverage grassland, and so forth. A:1990–1995 LULC change; B: 1995–2000 LULC change; C: 2000–2005 LULC change; D: 2005–2010 LULC change; E: 1990–2010 LULC change; R1: results of comparison of NCUE and FODS; R2: results of comparison of NCUE and LULC; R3: results of comparison of NCUE and NDVI. R4: results of comparison of NDVI and FODS; R5: results of comparison of NDVI and LULC.)

70 in 2009. Detailed information and comparison of results are shown in Table 3, Table 4 and Table 5.

Table 3 shows the information of all points and the results of the comparative analysis in 2013. The points with gray background are the ones where the land use type does not change during the1990-2010. Points which cannot express the trends of LULC type changes clearly are shown in bold, italic, and underlined fonts.

The comparative analysis results of the two periods in 2009 and 2013 are shown in Table 5. From Table 5, it is found that the performance of

NCUE is better than that of NDVI. Comparison with Field observed degradation situation, the performance of NCUE and NDVI is similar; For LUCC, the performance of NCUE is better than that of NDVI. The positive and negative change trend consistency between NDVI and NCUE is about 70%.

From Fig. 4 and Fig. 6, we can see that from the perspective of the positive and negative trends of the overall grassland change, the spatial distribution characteristic of NDVI and NCUE is similar. Yet, the biggest differences of change trends between NDVI and NCUE are that NDVI

**Table 4**  
Comparison of grassland changes detected by NCUE with field-observation data, LUCC and NDVI change trend in 2009 (partly listed).

ID	Latitude	Longitude	Field description	F	A	B	C	D	G	NDVI_S	NCUE_S	R1	R2	R3	R4	R5
1	34.36397	95.68698	black soil beach	UC	UC	UC	UC	UC		-0.0060705	-0.0098728	Y		Y	Y	
2	33.77107	95.7997	black soil beach	MC to LC	LC to MC	UC	UC	UC		0.0029256	0.0141897			Y		
3	32.89098	96.7422	small patches of black soil beach	UC	UC	UC	UC	UC		-0.005256	-0.0040255	Y		Y	Y	
4	<b>32.89788</b>	<b>96.63175</b>	<b>typical meadow, medium coverage</b>	UC	UC	MC to LC	UC	UC	DE	<b>-0.0033113</b>	<b>-0.0015831</b>	Y	Y	Y	Y	Y
5	<b>33.82122</b>	<b>97.14615</b>	<b>alpine meadow, partly wetland, medium coverage</b>	MC to LC	UC	UC	UC	UC	DE	<b>-0.0050478</b>	<b>-0.0040516</b>	Y	Y	Y	Y	Y
6	33.85003	97.19395	black soil beach on both sides of the road is more serious, there are small rivers	LC to MC	MC to BL	BL to LC	UC	UC		-0.0028885	-0.0070002	Y		Y	Y	
7	33.92538	97.28777	grassland degradation is severe, and there are swamp meadow	UC	UC	UC	UC	UC		-0.0006137	-0.0052494	Y		Y	Y	
8	<b>33.93032</b>	<b>97.29348</b>	<b>to the left of the road are large tracts of rat holes and early black soil beach</b>	MC to LC	UC	UC	UC	UC	DE	<b>0.0016295</b>	<b>-0.0101809</b>	Y	Y			
9	33.9378	97.30743	on the left side of the road is a swamp meadow, medium coverage	UC	MC to LC	LC to MC	UC	UC		0.0005539	-0.0065247	Y				
10	33.95727	97.3297	on the right side of the road, there is a swamp meadow and a small river, medium coverage	MC to LC	LC to MC	UC	UC	UC		0.0005126	-0.0057603	Y				

(Here: Points in bold font are LUCC comparison points. F means LULC change from 1980 to 1990; G means LULC change from 1980 to 2010; “black soil beach” means extremely degraded grassland.)

**Table 5**  
Comparative analysis consistency of changing trends in 2009 and 2013.

2013	2009		
	FODS	LULC	NDVI
NCUE	66.07%	68.00%	67.86%
NDVI	60.71%	64.00%	

detects more than 70% of the grassland showing significant changes, while NCUE only detects no more than 3%, and most of the areas are basically unchanged or in a state of insignificant changes. It shows that NDVI is sensitive to climate fluctuations, but NCUE overcomes the influence of climate fluctuations, reflecting the change of grassland being affected by human activities and long-term climate change. The grassland change detection result of NCUE is close to the existing researches (Wu et al. (2014); QUAYE-BALLARD, J.A. (2014)), yet the detection result of NDVI is completely different. Furthermore, it is found that counties in the east of TRHR showing large area grassland recovery in Fig. 6, but these areas belong to basically unchanged type shown in Fig. 7. This shows that the degree of insignificant restoration of grassland in the eastern part of the study area is lower than that of other place (such as Yushu), and the change is small over a long period of time, which is approximately unchanged.

## 5. Discussions

### 5.1. The characteristics of annual changes of major climatic factors and climatic factors selected

Thirteen meteorological stations in the study area were used to analyze statically the trends of the monthly average temperature, accumulation of rainfall, average hours of sunshine, average wind speed, etc. from 1982 to 2012. It was found that the annual average temperature of TRHR between 1982 and 2012 was  $-0.25\text{ }^{\circ}\text{C}$  and it

continued to increase at the rate of  $0.59\text{ }^{\circ}\text{C}/10\text{a}$ . The rising trend of the annual average temperature passed the significant test ( $p < 0.001$ ). Rainfall had significant inter-annual variations, and the overall increase was weak. Rainfall was mainly concentrated during the growing season, accounting for 82.3% of the rain throughout the whole year. The average hours of annual sunshine and the one during the growing season fluctuate greatly, and the overall trends are decreasing. These passed the significant level test ( $p < 0.05$ ). The annual average wind speed and the one during the growing season show clear downward trends and pass the significant test ( $p < 0.001$ ). The average annual surface temperature and the one during the growing season showed significant upward trends ( $p < 0.001$ ) from 1982 to 2012. In 1994, the surface temperature changed from cold to warm, and beyond 1997, it presents a clear increasing trend (Sun, 2015).

The thirteen meteorological factors selected based on the data from weather stations and Pearson correlation analysis are as follows: the sum of the precipitation during the growing season, the average of the temperature, sunshine hours, surface temperature, and wind speed of growing season; three hysteresis effect factors including the average surface temperature in April, the average wind speed in March and the average surface temperature in February; and other factors including an annual accumulated temperature of greater than  $0\text{ }^{\circ}\text{C}$ , the growth season rainfall condition index, the temperature condition index, the sunshine conditions index and the STPC index. Freeze and thaw are important factor that affect the soil moisture in the TRHR region, and they will be considered in future study.

### 5.2. The modeling effect of the IMF

Multiple linear stepwise regression (backward mode) and five climatic factors of the growing season, including the accumulative precipitation, average temperature, average sunshine, average land surface temperature and average wind speed, excluding time-lag effects, were used in the model, and the effective model is established on each weather station. On average, the correlation coefficient was 0.53 with low estimation accuracy. A more effective model could be established for each site after adding time-lag effects and hydrothermal combinations of variables. The correlation coefficient could reach 0.68 on average.

By performing multiple stepwise linear regressions, taking the NDVI as a dependent variable and climate factors as independent variables, it was found that the incorporation of more independent variables does not necessarily produce a good modeling effect. Too many parameters could cause overfitting and collinearity problems among different variables, while too few will also affect the modeling accuracy. When the multivariate regression was employed with the “Enter” mode, it was found that the majority of sites were unable to establish an effective model of the accumulated NDVI and climatic elements. In contrast, Stepwise regression could establish the relevant model effectively, and it passed the significant level test ( $p < 0.05$  at 95% confidence interval). The few factors selected during the modeling process could reflect the major factors, but the modeling accuracy is relatively low, with the average correlation coefficient of 0.48 only. “Backward” mode selects moderate parameters with high modeling accuracy. However, there are some sites with too many parameters, while some of the independent variables were strongly correlated. It is worth paying attention to the choice of the appropriate number of factors to reach a high precision of modeling without overfitting to avoid collinearity. After the first multiple linear regression we will check the collinearity problem, such as whether the VIF (Variance Inflation Factor) is greater than 10 or the Condition Index is greater than 30. If these situations occur, then the independent variable corresponding to the largest VIF or the Condition Index will be removed. The remaining independent variables will be used for the re-regression. This can solve the problem of collinearity between independent variables. Experiments in meteorological stations illustrate the effectiveness of the method.

### 5.3. Analysis of effectiveness of NCUE

Correlation analysis was carried out between each factor within the NCUE to illustrate that the NCUE presented in this paper is effective for reducing climatic fluctuation. The spatial distribution of the correlation

coefficient between the NCUE and IMF is shown in Fig. 8. It was found that the correlation between the NCUE and IMF was weak, and in most areas, their correlation did not pass the significant test of 0.05. This result shows that NCUE can reduce the influence of climate fluctuation. The correlation between the cumulative NDVI during the growing season and the IMF was high, and the NDVI is greatly affected by the climate. The correlation between the cumulative NDVI and the NCUE during the growing season was also significant, and the NCUE can reflect vegetation growth well, which is not sensitive to climate fluctuations (Fig. 8).

### 5.4. Credibility analysis of the results of detected grassland changes

The results were comparatively analyzed using field surveys, LUC and NDVI changes. Four kinds of grassland change data can be used for comparative analysis. These can reflect the states and changes in grassland vegetation. The long-term changes of grassland observed through field surveys are conceptually different from the monitoring of grassland degradation in this paper. However, there might be some relationships between the results of the changes and the process of the changes. Therefore, there may be some rationality behind the analysis and comparison.

It is feasible to perform a comparative analysis using the five sets of LULC changes because there is consistency in the classification definitions. There are some differences in the essence between these four kinds of grassland change detection methods (which are field survey, LUC comparison, NDVI and NCUE), and this will produce a certain uncertainty in the analysis results. Observations in the field are the result of long-term changes in grassland. The coverage and community structure information were considered in the classification of the grassland degradation level, reflecting the objective reality of the degraded grassland.

The NCUE slope reflects the long-term trends of vegetation growth after reducing the impact of climate fluctuation. The LULC changes also reflect the long-term trends of vegetation growth. The change of the total vegetation cover does not reflect the changes in the community structure and does not take the impact of climate fluctuation into account. In addition, the LULC data is obtained from visual interpretation through human-computer interactions. The complexity of natural phenomena, such as grassland degradation, as well as the domain knowledge and the subjectivity of the interpreter, may all lead to uncertainty in the identification. Due to the lack of long-term fixed-point field observation data and certain errors in the various types of data used in the analysis, the results present some uncertainties. It is necessary to obtain more reliable data to strengthen the analysis and verification of

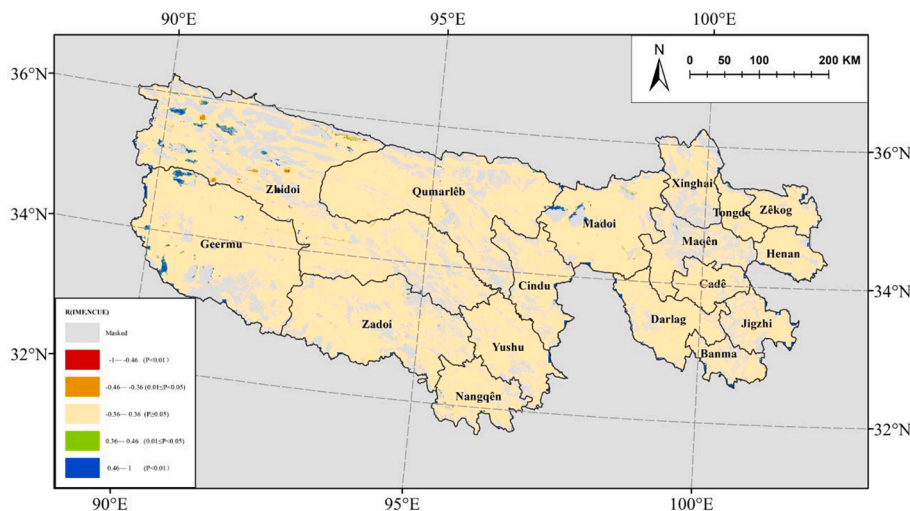


Fig.8. Correlation coefficient and significance test between NCUE and IMF.

**Table 6**  
Some previous studies of the grassland restoration and degradation in TRHR.

Reference	Indicators	Time span	Remote sensing data	Results of grassland restoration and degradation
This study	NUCE	1982-2012	NOAA / AVHRR-NDVI MODIS-NDVI	Overall trend: a slightly recovery trend. Degradation concentrated distribution areas: northeast of Maduo, midwest of Qumarlèb and Zhidoi and the Geermu local area, et al. Restoration concentrated distribution areas: In the central Yushu and Nangqên County, Qumarlèb, Zhidoi, Zadoi County, et al.; the southeast of TRHR, such as Jigzhi, Darlag et al.
Liu et al.(2008)	Coverage change rate, grassland fragmentation, etc.	Mid to late 1970 s, early 1990 s, 2004	MSS, TM, TM/ETM	Overall trend: the continued process of grassland degradation. Degradation concentrated distribution areas: Qumarlèb, Chenduo, Maduo, et al. Restoration concentrated distribution areas: in Zadoo and Tanggula Mountain Township, the grassland has local improvement areas.
Wuet al.(2014)	reference vegetation coverage	1981–2006	NOAA / AVHRR-NDVI	Overall trend: no major development in grassland degradation since 1980 s. After 2000, the grassland degradation trend was slowed down initially. Degradation concentrated distribution areas: Zadoo, Dari, Qumarlèb, Tanggula Mountain Township, Xinghai, Maduo, et al. Less degraded areas: Gander, Zeku, Henan, Tongde, et al.
QUAYE-BALLARD, J.A. 2014)	A <sub>5</sub> time series produced by Multi-Resolution Analysis (MRA) of Wavelet Transform	1981–2012	NOAA / AVHRR-NDVI MODIS-NDVI	Overall trend: The total ratios of the positive and negative slopes are 69.6% and 30.4%. Degradation concentrated distribution areas: Qumarlèb, Chenduo, Maduo, et al. Restoration concentrated distribution areas: in Zadoo and Tanggula Mountain Township, the grassland has local improvement areas.
Shenet al.(2018)(	Detecting Breakpoints and Estimating Segments in Trend(DBEST)	2000-2015	MODIS-NDVI	Overall trend: recovery of the vegetation. Degradation concentrated distribution areas: Maduo, Zadoi, Nangqên, Jiuzhi and Zhidoi, et al. Restoration concentrated distribution areas: the southeastern TRHR, including Xinghai, Tongde, Zeku, as well as the middle regions, such as Chengduo and Yushu, et al.

the results. Additionally, the size of the field survey samples is  $30 \times 30$  square meters. Since the pixel size used in this paper is  $250 \times 250$  square meters, there might be some discrepancies caused by the inconsistency in spatial scales when analyzing based on field observations.

The research found that the correlation between the cumulative NDVI and cumulative rainfall is very weak at pixel scale, so the RUE index that only considers rainfall factors may not characterize NDVI well. Therefore, the RUE and the Residual Index derived by RUE are also not used in this article. This article compares the temporal trends of cumulative NDVI during the growing season and NCUE.

A comparison with some previous studies of the grassland restoration and degradation in TRHR are shown in Table 6. The period of these studies is close to or partially overlaps with this study.

It is found that the grassland showed a recovery trend in this study, and which is basically consistent with that of Wu et al. (2014), Quaye-Ballardq (2014), and Shen et al. (2018). The proportions of unchanged and significantly change grassland are similar to that of Quaye-Ballardq (2014). Degradation area is between that of Liu et al. (2008) and Wu et al. (2014). Restoration area in this study is slightly higher than that of 1990 s – 2000 s later (Wu et al., 2014). For degradation concentrated distribution areas in the paper, there is more overlap with the conclusions of other studies. Restoration concentrated distribution areas are similar to that of Wu et al. (2014) and Shen et al. (2018).

Form Table 6, it is found that there is a certain degree of difference between the results of the various studies because of different grassland degradation indicators, method mechanism, research periods, and data accuracy, etc. These differences should hinder the comparison between the results of different studies in the same area.

Results may hide the severity of grassland degradation when using the NDVI method. Grassland degradation is shown not only as a decrease in biomass or coverage but also as changes in the composition of the community. In the early stage of grassland degradation, obvious changes of biomass usually do not occur, but there are changes in the community structure, where the reduction of dominant native grass species appears with the increase of poisonous weeds. In some severely degraded areas, the vegetation coverage is low, and there are large areas of bare land. However, in other severely degraded areas, a large number of poisonous weeds may grow with high coverage. Using the grassland NDVI alone as

a deteriorating indicator, it will be impossible to distinguish between these situations. A field investigation found that poisonous weeds breed quickly in the TRHR. They also mix with native plant species. Poisonous weeds grow well and cover large areas of vegetation in the extremely degraded “Black Earth Beach” area, and few native plant species exist. This type of situation will cover up the actual degree of grassland degradation and lead to uncertainty in the monitoring of grassland degradation using the NDVI time series method.

## 6. Conclusion

Inspired by the RUE and based on the climate characteristics of the study area, a novel grassland ecosystem characteristic index, the NCUE, was proposed in this paper through the comprehensive consideration of major climatic factors affecting the growth of grassland vegetation, such as light, temperature, and water, using multi-source geospatial data. The model was adapted for the monitoring of grassland changes in the study area and could reduce the influence of climate fluctuations. Through analysis and comparison with actual observed data, land use/cover data and NDVI, the NCUE index was shown to be effective in monitoring grassland changes.

Most of the grasslands in the TRHR have shown insignificantly changes in the past 31 years. At the same time, grassland degradation and restoration co-exist, and the area of degraded grassland is slightly less than that of restored grassland. In terms of spatial distribution in grassland changes, there is a trend of restoration in the southeast and middle region and degradation in the northwest based on the positive and negative change trends. There are large areas of grassland restoration in the southeastern part of Jiuzhi, Darlag Counties, as well as in Yushu, Nangqian, Qumarlèb and Zhidoi Counties in the TRHR. Grassland degradation is mainly distributed in the northeast of Maduo County and the central and western parts of Zhidu County, Qumarlèb, and Golmud. The NCUE might be applied in similar arid and semi-arid alpine grassland areas (such as in Gansu Province, the Ningxia Hui Autonomous Region, the Tibet Autonomous Region, etc.).

Due to the cold weather and harsh natural conditions in this area, it is difficult to conduct field surveys. Due to the lack of long-term fix-point field observation data and the various data used for the analysis, the

results may present some uncertainty. We should further acquire more reliable data sources to strengthen the analysis and verification of monitoring results. In the future, we would like to strengthen the research of information extraction on large-scale weeds and perform more scientific monitoring of grassland degradation. The reason and mechanism of grassland degradation in this area should further be studied to evaluate the effectiveness of environmental protection and human activities objectively. Grassland degradation can also cause soil degradation and even desertification; changes in grassland seed bank and soil properties, such as soil water content, soil organic carbon, total nitrogen and soil bulk density, soil microorganisms, soil enzyme, etc. In the future, we can also conduct research on soil degradation, desertification, and changes in soil moisture caused by grassland degradation with the help of remote sensing technology.

#### CRediT authorship contribution statement

**Ru An:** Writing – original draft, Conceptualization, Validation, Formal analysis, Investigation. **Ce Zhang:** Methodology, Writing – review & editing, Supervision, Project administration. **Mengqiu Sun:** Writing – review & editing, Investigation. **Huilin Wang:** Writing – review & editing, Validation, Project administration. **Xiaoji Shen:** Methodology, Writing – review & editing. **Benlin Wang:** Writing – review & editing, Validation. **Fei Xing:** Writing – review & editing, Investigation. **Xianglin Huang:** Writing – review & editing, Investigation. **Mengyao Fan:** Writing – review & editing, Formal analysis.

#### Declaration of Competing Interest

The authors declare that they have no known competing financial interests or personal relationships that could have appeared to influence the work reported in this paper.

#### Acknowledgments

This work is supported by the National Nature Science Foundation of China (No. 41271361; 41871326). The authors would like to express sincere gratitude to X.Z. Feng from the Nanjing University, J.Y. Liu, Q.Q. Shao, J.W. Fan from the Institute of Geography Sciences and Natural Resources Research (CAS), and Y. Wang from the University of Warwick, UK for their suggestions and assistance with the provision of research data.

#### References

- An, R., Wang, H.L., Feng, X.-Z., Wu, H., Wang, Z., Wang, Y., Shen, X.J., Lu, C.H., Quayeballard, J.A., Chen, Y.-H., Zhao, Y.-H., 2017. Monitoring rangeland degradation using a novel local NPP scaling based scheme over the “Three-River Headwaters” region, hinterland of the Qinghai-Tibetan Plateau. *Quat. Int.* 444, 97–114. <https://doi.org/10.1016/j.quaint.2016.07.050>.
- An, R., Xu, X.F., Yang, R.M., 2014. Time-Lag Effect of Vegetation NDVI on Regional Climate in “Three River Source” Region. *Geomatics Spat. Inf. Technol.* 37, 1–5.
- Bai, Z.G., Dent, D.L., Olsson, L., Schaeppman, M.E., 2008. Proxy global assessment of land degradation. *Soil Use Manag.* 24, 223–234. <https://doi.org/10.1111/j.1475-2743.2008.00169.x>.
- Bastin, G., Scarth, P., Chewings, V., Sparrow, A., Denham, R., Schmidt, M., O’Reagan, P., Shepherd, R., Abbott, B., 2012. Separating grazing and rainfall effects at regional scale using remote sensing imagery: A dynamic reference-cover method. *Remote Sens. Environ.* 121, 443–457. <https://doi.org/10.1016/j.rse.2012.02.021>.
- Brown de Colstoun, E., Kravitz, L.L., Prince, S.D., 1998. Evidence from rain-use efficiencies does not indicate extensive Sahelian desertification. *Glob. Chang. Biol.* 4, 359–374. <https://doi.org/10.1046/j.1365-2486.1998.00158>.
- Burrell, A.L., Evans, J.P., Liu, Y., 2017. Detecting dryland degradation using Time Series Segmentation and Residual Trend analysis (TSS-RESTREND). *Remote Sens. Environ.* 197, 43–57. <https://doi.org/10.1016/j.rse.2017.05.018>.
- Cai, H., Yang, X., Xu, X., 2015. Human-induced grassland degradation/restoration in the central Tibetan Plateau: The effects of ecological protection and restoration projects. *Ecol. Eng.* 83, 112–119. <https://doi.org/10.1016/j.ecoleng.2015.06.031>.
- Chen, Q., Zhou, Q., Zhang, H.F., Liu, F.G., 2010. Spatial disparity of NDVI response in vegetation growing season to climate change in the Three-River Headwaters Region. *Ecol. Environ. Sci.* 19, 1284–1289.
- de Jong, R., de Bruin, S., de Wit, A., Schaeppman, M.E., Dent, D.L., 2011. Analysis of monotonic greening and browning trends from global NDVI time-series. *Remote Sens. Environ.* 115 (2), 692–702. <https://doi.org/10.1016/j.rse.2010.10.011>.
- Eckert, Sandra, Hülsler, Fabia, Liniger, Hanspeter, Hodel, Elias, 2015. Trend analysis of MODIS NDVI time series for detecting land degradation and regeneration in Mongolia. *J. Arid Environ.* 113, 16–28.
- Eddy, I.M.S., Gergel, S.E., Coops, N.C., Henebry, G.M., Levine, J., Zerriffi, H., Shirkov, E., 2017. Integrating remote sensing and local ecological knowledge to monitor rangeland dynamics. *Ecol. Indic.* 82, 106–116. <https://doi.org/10.1016/j.ecolind.2017.06.033>.
- Evans, J., Geerken, R., 2004. Discrimination between climate and human-induced dryland degradation. *J. Arid Environ.* 57 (4), 535–554. [https://doi.org/10.1016/S0140-1963\(03\)00121-6](https://doi.org/10.1016/S0140-1963(03)00121-6).
- Fensholt, R., Langanke, T., Rasmussen, K., Reenberg, A., Prince, S.D., Tucker, C., Scholes, R.J., Le, Q.B., Bondeau, A., Eastman, R., Epstein, H., Gaughan, A.E., Hellden, U., Mbow, C., Olsson, L., Paruelo, J., Schweitzer, C., Seauist, J., Wessels, K., 2012. Greenness in semi-arid areas across the globe 1981–2007 - an Earth Observing Satellite based analysis of trends and drivers. *Remote Sens. Environ.* 121, 144–158. <https://doi.org/10.1016/j.rse.2012.01.017>.
- Fu, B.P., 1983. *Mountain climate*. Science Press, Beijing.
- Gao, J.G., Zhang, Y.L., Liu, L.S., Wang, Z.F., 2014. Climate change as the major driver of alpine grasslands expansion and contraction: A case study in the Mt. Qomolangma (Everest) National Nature Preserve, southern Tibetan Plateau. *Quat. Int.* 336, 108–116. <https://doi.org/10.1016/j.quaint.2013.09.035>.
- Gao, Z.H., Li, Z.Y., Ding, G.D., Li, L.Y., 2005. New approach for desertification assessment by remote sensing based upon Rain Use Efficiency of vegetation. *Sci. Soil Water Conserv.* 3, 37–41.
- Gardiner, B., Berry, P., Moulia, B., 2016. Review: Wind impacts on plant growth, mechanics and damage. *Plant Sci.* 245, 94–118. <https://doi.org/10.1016/j.plantsci.2016.01.006>.
- Geerken, R., Ilaiwi, M., 2004. Assessment of rangeland degradation and development of a strategy for rehabilitation. *Remote Sens. Environ.* 90 (4), 490–504. <https://doi.org/10.1016/j.rse.2004.01.015>.
- Gu, Z.H., Shi, P.J., Chen, J., 2010. Estimation of grassland degradation based on maximum response of vegetation to climate. *J. Nat. Disasters* 19, 13–20.
- Harris, R.B., 2010. Rangeland degradation on the Qinghai-Tibetan plateau: A review of the evidence of its magnitude and causes. *J. Arid Environ.* 74 (1), 1–12. <https://doi.org/10.1016/j.jaridenv.2009.06.014>.
- Holben, Brent, N., 1986. Characteristics of maximum-value composite images from temporal AVHRR data. *Int. J. Remote Sens.* 7 (11), 1417–1434.
- Holm, A.M.R., Cridland, S.W., Roderick, M.L., 2003. The use of time-integrated NOAA NDVI data and rainfall to assess landscape degradation in the arid shrubland of Western Australia. *Remote Sens. Environ.* 85, 145–158. [https://doi.org/10.1016/S0034-4257\(02\)00199-2](https://doi.org/10.1016/S0034-4257(02)00199-2).
- Houérou, L., Henri, N., 1984. Rain use-efficiency: a unifying concept in arid-land ecology. *J. Arid Environ.* 7, 213–247.
- Huang, Q.X., Zhao, Y., He, Q., 2013. Climatic Characteristics in Central Asia Based on CRU Data. *Arid Zo. Res.* 30, 396–403.
- He, J., Yang, K., Tang, W., Liu, H., Qin, J., Chen, Y.Y., Li, X., 2020. The first high-resolution meteorological forcing dataset for land process studies over China. *Sci. Data* 7 (1), 25. <https://doi.org/10.1038/s41597-020-0369-y>.
- Karnieli, A., Bayarjargal, Y., Bayasgalan, M., Mandakh, B., Dugarjav, C.H., Burgheimer, J., Khudulmur, S., Bazha, S.N., Gunin, P.D., 2013. Do vegetation indices provide a reliable indication of vegetation degradation? A case study in the Mongolian pastures. *Int. J. Remote Sens.* 34 (17), 6243–6262. <https://doi.org/10.1080/01431161.2013.793865>.
- Leroux, L., Bégué, A., Lo Seen, D., Jolivot, A., Kayitakire, F., 2017. Driving forces of recent vegetation changes in the Sahel: Lessons learned from regional and local level analyses. *Remote Sens. Environ.* 191, 38–54. <https://doi.org/10.1016/j.rse.2017.01.014>.
- Li, A., Wu, J., Huang, J., 2012. Distinguishing between human-induced and climate-driven vegetation changes: A critical application of RESTREND in inner Mongolia. *Lands. Ecol.* 27 (7), 969–982. <https://doi.org/10.1007/s10980-012-9751-2>.
- Li, B., 1997. *The Rangeland Degradation in North China and Its Preventive Strategy*. *Sci. Agric. Sin.* 30, 1–9.
- Li, C.X., de Jong, R., Schmid, B., Wulf, H., Schaeppman, M.E., 2020a. Changes in grassland cover and in its spatial heterogeneity indicate degradation on the Qinghai-Tibetan Plateau. *Ecolog. Indicators* 119 (106641), 1–12.
- Li, L., Li, F.-X., Guo, A.-H., Al, E., 2006. Study on the Climate Change Trend and Its Catastrophe over “The Source Region of Three Rivers” Region in Recent 43 Years. *J. Nat. Resour.* 21, 79–85.
- Li, N., Zhan, P., Pan, Y., Zhu, X., Li, M., Zhang, D., 2020b. Comparison of remote sensing time-series smoothing methods for grassland spring phenology extraction on the Qinghai-Tibetan plateau. *Remote Sens.* 12, 1–26. <https://doi.org/10.3390/rs12203383>.
- Liu, J., Xu, X., Shao, Q., 2008. The spatial and temporal characteristics of grassland degradation in the three-river headwaters region in Qinghai Province. *Acta Geogr. Sin.* 63, 364–376.
- Liu, M.C., Li, D.Q., Luan, X.F., Wen, Y.M., 2005. Ecosystem services and its value evaluation of San Jiang Yuan Region. *J. Plant Resour. Environ.* 14, 40–43.
- Lu, L., 2011. *Study on Grassland Degradation Monitoring in the Source of Three Rivers considering the impact of climate fluctuations*. Hohai University.
- Lu, Z.Y., Cai, F., Liu, W.M., Yuan, Z.P., Chen, Y.Q., Chen, M.Q., 2009. Spatial interpolation methods of wind relative humidity and cloud cover in villages and towns weather forecast in Liaoning province. *J. Meteorol. Environ.* 25, 54–57.

- Meroni, M., Schucknecht, A., Fasbender, D., Rembold, F., Fava, F., Mauclair, M., Goffner, D., Di Lucchio, L.M., Leonardi, U., 2017. Remote sensing monitoring of land restoration interventions in semi-arid environments with a before–after control–impact statistical design. *Int. J. Appl. Earth Obs. Geoinf.* 59, 42–52. <https://doi.org/10.1016/j.jag.2017.02.016>.
- Nicholson, S.E., Tucker, C.J., Ba, M.B., 1998. Desertification, drought, and surface vegetation: An example from the West African Sahel. *Bull. Am. Meteorol. Soc.* 79, 815–829. [https://doi.org/10.1175/1520-0477\(1998\)079<0815:DDASVA>2.0.CO;2](https://doi.org/10.1175/1520-0477(1998)079<0815:DDASVA>2.0.CO;2).
- Pan, D.F., 2007. Study on the Types and Grades of “Black Soil Type” Degraded Grassland in the Sanjiangyuan Region. Gansu Agricultural University.
- Prince, S.D., 2012. Mapping Desertification in Southern Africa, in: G.Gutman, A.Janetos, C.O.Justice, E.F.Moran, J.F.Mustard, R.Rindfuss, D.Skole, B.L.Turner (Eds.), *Land Change Science: Observing, Monitoring, and Understanding Trajectories of Change on the Earth’s Surface*. Springer, Berlin, pp. 163–184. [https://doi.org/10.1007/978-1-4020-2562-4\\_10](https://doi.org/10.1007/978-1-4020-2562-4_10).
- Prince, S.D., Becker-Reshef, I., Rishmawi, K., 2009. Detection and mapping of long-term land degradation using local net production scaling: Application to Zimbabwe. *Remote Sens. Environ.* 113 (5), 1046–1057. <https://doi.org/10.1016/j.rse.2009.01.016>.
- Qian, Shuan, Fu, Yang, Pan, FeiFei, 2010. Climate change tendency and grassland vegetation response during the growth season in Three-River Source Region. *Sci. China Earth Sci.* 53 (10), 1506–1512. <https://doi.org/10.1007/s11430-010-4064-2>.
- Qian, S., Mao, L.X., Zhang, Y.H., 2007. Evaluation models of meteorological conditions for vegetation growth on natural grasslands in China. *Chinese J. Ecol.* 26, 1499–1504.
- Quaye-Ballardq, J.A., 2014. Drought Impact Assessment on Rangeland Degradation at the Source Region of Yangtze. Hohai University, Yellow and Lancang Rivers.
- Seaquist, J.W., Hickler, T., Eklundh, L., Ardö, J., Heumann, B.W., 2008. Disentangling the effects of climate and people on Sahel vegetation dynamics. *Biogeosciences Discuss.* 5, 3045–3067. <https://doi.org/10.5194/bgd-5-3045-2008>.
- Shen, X., An, R., Feng, L., Ye, N., Zhu, L., Li, M., 2018. Vegetation changes in the Three-River Headwaters Region of the Tibetan Plateau of China. *Ecol. Indic.* 93, 804–812. <https://doi.org/10.1016/j.ecolind.2018.05.065>.
- Stow, Douglas A, Hope, Allen, McGuire, David, Verbyla, David, Gamon, John, Huemrich, Fred, Houston, Stan, Racine, Charles, Sturm, Matthew, Tape, Kenneth, Hinzman, Larry, Yoshikawa, Kenji, Tweedie, Craig, Noyle, Brian, Silapaswan, Cherie, Douglas, David, Griffith, Brad, Jia, Gensuo, Epstein, Howard, Walker, Donald, Daeschner, Scott, Petersen, Aaron, Zhou, Liming, Myneni, Ranga, 2004. Remote sensing of vegetation and land-cover change in Arctic Tundra Ecosystems. *Remote Sens. Environ.* 89 (3), 281–308. <https://doi.org/10.1016/j.rse.2003.10.018>.
- Sun, M.Q., 2015. Temporal and spatial pattern of rangeland degradation and its influence factors for the Three River Headwaters Region from 1982 to 2012. Hohai University.
- Verón, S.R., Paruelo, J.M., Oesterheld, M., 2006. Assessing desertification. *J. Arid Environ.* 66 (4), 751–763. <https://doi.org/10.1016/j.jaridenv.2006.01.021>.
- Vetter, S., 2005. Rangelands at equilibrium and non-equilibrium: Recent developments in the debate. *J. Arid Environ.* 62 (2), 321–341. <https://doi.org/10.1016/j.jaridenv.2004.11.015>.
- Wang, J., Li, W.J., Song, D.M., Tang, H., Dong, G.R., 2004. The analysis of land desertification changing of Minqin County in recent 30 years. *J. Remote Sens.* 8, 282–288.
- Wang, K., 2004. Grassland restoration and reconstruction. Chemical Industry Press, Beijing.
- Wang, S.W., Yi, G.H., Gao, Y.P., Zhang, T.B., Bie, X.J., 2014. The research of quantitative relationship between land surface temperature and land cover in Three-River Source Region based on MODIS data. *Geomatics Spat. Inf. Technol.* 37, 56–61.
- Wessels, K.J., Prince, S.D., Malherbe, J., Small, J., Frost, P.E., VanZyl, D., 2007. Can human-induced land degradation be distinguished from the effects of rainfall variability? A case study in South Africa. *J. Arid Environ.* 68 (2), 271–297. <https://doi.org/10.1016/j.jaridenv.2006.05.015>.
- Wessels, K.J., Prince, S.D., Reshef, I., 2008. Mapping land degradation by comparison of vegetation production to spatially derived estimates of potential production. *J. Arid Environ.* 72 (10), 1940–1949. <https://doi.org/10.1016/j.jaridenv.2008.05.011>.
- Wu, Z., Li, F., Zhang, L., Zhang, J., Du, J., 2014. Research on grassland degradation of Three-river Headwaters Region based on reference vegetation coverage. *J. Nat. Disasters* 23, 94–102. <https://doi.org/10.13577/j.jnd.2014.0213>.
- Xu, D.Y., Kang, X.W., Zhuang, D.F., Pan, J.J., 2010. Multi-scale quantitative assessment of the relative roles of climate change and human activities in desertification - A case study of the Ordos Plateau. *China. J. Arid Environ.* 74 (4), 498–507. <https://doi.org/10.1016/j.jaridenv.2009.09.030>.
- Xue, Xian, Guo, Jian, Han, Bangshuai, Sun, Qingwei, Liu, Lichao, 2009. The effect of climate warming and permafrost thaw on desertification in the Qinghai-Tibetan Plateau. *Geomorphology* 108 (3-4), 182–190. <https://doi.org/10.1016/j.geomorph.2009.01.004>.
- Yan, Y., 2008. Differentiation of related concepts of grassland degradation. *Acta Prataculturae Sin.* 17, 93–99.
- Yang, R.M., 2012. Research on ecosystem function indicator for vegetation degradation detection in the “Three River Headwaters Region. Hohai University.
- Yu, H., 2013. Dynamics of Grassland Growth and Its Response to Climate Change on Tibetan Plateau. Lanzhou University.
- Yu, X.Y., Shao, Q.Q., Liu, J.Y., 2012. Spectral analysis of different degradation level alpine meadows in “Three-river headwaters” region. *Chinese J. Geo-Information Sci.* 14, 398–404.
- Zhang, Y., Zhang, C. Bin, Wang, Z.Q., Yang, Y., Zhang, Y.Z., Li, J.L., An, R., 2017a. Quantitative assessment of relative roles of climate change and human activities on grassland net primary productivity in the Three-River Source Region. *China. Acta Prataculturae Sin.* 26, 1–14. <https://doi.org/10.11686/cyxb2016420>.
- Zhang, Y.X., Fan, J.W., Cao, W., Zhang, H.Y., 2017b. Spatial and temporal dynamics of grassland yield and its response to precipitation in the Three River Headwater Region from 2006 to 2013. *Acta Prataculturae Sin.* 26, 10–19. <https://doi.org/10.11686/cyxb2017008>.
- Zhao, F., 2012. Temporal and spatial variation and driving factors analysis of vegetation index (MODIS NDVI/EVI) of grasslands in the Three-Rivers Headwaters region. Qinghai University.
- Zika, Michael, Erb, Karl-Heinz, 2009. The global loss of net primary production resulting from human-induced soil degradation in drylands. *Ecol. Econ.* 69 (2), 310–318. <https://doi.org/10.1016/j.ecolecon.2009.06.014>.